Radiotherapy and Oncology 175 (2022) 203–209

Contents lists available at ScienceDirect

Radiotherapy and Oncology

journal homepage: www.thegreenjournal.com

Original Article

Design and validation of a dosimetric comparison scheme tailored for ultra-high dose-rate electron beams to support multicenter FLASH preclinical studies

Patrik Gonçalves Jorge [b], Stavros Melemenidis [c], Veljko Grilj [b], Thierry Buchillier [b], Rakesh Manjappa [c], Vignesh Viswanathan [c], Maude Gondré [b], Marie-Catherine Vozenin [a], Jean-François Germond [b], François Bochud [b], Raphaël Moeckli [b], Charles Limoli [e], Lawrie Skinner [c], Hyunsoo Joshua No [c], Yufan Fred Wu [c], Murat Surucu [c], Amy S. Yu [c], Brianna Lau [c], Jinghui Wang [c,1], Emil Schüler [d], Karl Bush [c,1], Edward E. Graves [c], Peter G. Maxim [e], Billy W. Loo Jr [c], Claude Bailat [b,*]

[a] *CHUV – Radiation-oncology Laboratory;* [b] *Institute of Radiation Physics, Lausanne University Hospital and University of Lausanne, Lausanne, Switzerland;* [c] *Department of Radiation Oncology, Stanford University School of Medicine, Stanford, CA 94305;* [d] *Department of Radiation Physics, MD Anderson Cancer Center, Houston, TX 77030; and* [e] *Department of Radiation Oncology, University of California, Irvine, CA 92697, USA*

ARTICLE INFO

Article history:
Received 29 March 2022
Received in revised form 18 August 2022
Accepted 19 August 2022
Available online 27 August 2022

Keywords:
UHDR
FLASH
Dosimetry
Intercomparison
Passive dosimeters

ABSTRACT

Background and purpose: We describe a multicenter cross validation of ultra-high dose rate (UHDR) (>= 40 Gy/s) irradiation in order to bring a dosimetric consensus in absorbed dose to water. UHDR refers to dose rates over 100–1000 times those of conventional clinical beams. UHDR irradiations have been a topic of intense investigation as they have been reported to induce the FLASH effect in which normal tissues exhibit reduced toxicity relative to conventional dose rates. The need to establish optimal beam parameters capable of achieving the *in vivo* FLASH effect has become paramount. It is therefore necessary to validate and replicate dosimetry across multiple sites conducting UHDR studies with distinct beam configurations and experimental set-ups.

Materials and methods: Using a custom cuboid phantom with a cylindrical cavity (5 mm diameter by 10.4 mm length) designed to contain three type of dosimeters (thermoluminescent dosimeters (TLDs), alanine pellets, and Gafchromic films), irradiations were conducted at expected doses of 7.5 to 16 Gy delivered at UHDR or conventional dose rates using various electron beams at the Radiation Oncology Departments of the CHUV in Lausanne, Switzerland and Stanford University, CA.

Results: Data obtained between replicate experiments for all dosimeters were in excellent agreement (±3%). In general, films and TLDs were in closer agreement with each other, while alanine provided the closest match between the expected and measured dose, with certain caveats related to absolute reference dose.

Conclusion: In conclusion, successful cross-validation of different electron beams operating under different energies and configurations lays the foundation for establishing dosimetric consensus for UHDR irradiation studies, and, if widely implemented, decrease uncertainty between different sites investigating the mechanistic basis of the FLASH effect.

Normal tissue protection in radiation therapy (RT) has been greatly improved over recent decades thanks to increased accuracy in the delivered dose, improved dose conformity, and fractionation [1–4]. Recently, multiple preclinical studies have shown that the use of ultra-high dose-rate (UHDR) beams under specific configurations can trigger the "FLASH effect", which increases the differential response between normal tissues and tumors when compared to conventional dose-rate (CONV) RT. This may provide an opportunity for dose escalation with curative intent while minimizing dose limiting toxicities [5–9]. Since the underlying mechanisms behind the FLASH effect are still not fully understood [9–13], additional preclinical studies must be conducted with accurate and reproducible measurements to safely and properly evaluate the translational potential of FLASH-RT.

* Corresponding author at: Institute of Radiation Physics, Rue du Grand-Pré 1, CH-1007 Lausanne, Switzerland.
E-mail address: Claude.bailat@chuv.ch (C. Bailat).
[1] Current affiliation: Varian Medical Systems, Palo Alto, CA 94304, USA.

https://doi.org/10.1016/j.radonc.2022.08.023
0167-8140/

The dose-per-pulse and dose-rate within the pulse of UHDR beams are several orders of magnitude larger than those in CONV-RT. However, International Codes of Practice do not provide metrological protocols for absorbed dose determination under these conditions [14,15]. Neither primary standards nor validated UHDR beams from National Metrology Institutes (NMI) are available [16]. Additionally, no formalism and no reference conditions have yet been established for UHDR beams. As a result, traceability is not currently directly or reliably achievable.

To overcome the lack of traceability, UHDR dosimetry has been developed over the years at CHUV on a redundant metrological scheme using alanine, radiochromic films, and thermoluminescent dosimeters (TLDs). One study demonstrated a compatible dose–response relationship from all dosimeters over the range from CONV to UHDR with MeV electrons [17] while other studies investigated the dose-rate dependency of these dosimeters independently [18–24].

Within the current framework, a step forward is to rigorously establish traceability through interlaboratory comparisons in order to bring a dosimetric consensus.

Quality assurance in dosimetric standardization is particularly critical for large collaborative projects, where consistent and reproducible irradiation conditions are necessary prerequisites to interpret and advance UHDR biological studies conducted at different locations. Typically, radiobiological studies performed in parallel at various locations are based on a shared understanding of absorbed dose to water dosimetry and its chain of traceability. The absorbed dose to water is the most used metric in order to compare radiobiological results. Other beam metrics may assume greater importance as our understanding of critical FLASH beam parameters increases over time, but currently, the milestone physical quantity used for comparison remains the absorbed dose to water [9,25,26].

Consequently, this work presents the design and validation of a comparison scheme, aiming to obtain a dosimetric consensus as well as a cross validation among UHDR facilities. Contrary to most interlaboratory comparisons, our scheme has no adequate metrological traceability to a primary standard, which is one of the goals of the UHDpulse project [16]. We tried to cover a large spectrum of irradiation conditions and parameters, typically, in term of dose rate and beam geometry. In addition, we tried take advantage of the two location by developing the scheme at CHUV and testing its feasibility at Stanford.

Materials and methods

Cuboid phantom

Fig. 1 shows the cuboid phantom (25 × 25 × 32 mm^3) made of acrylic (PMMA, ρ = 1.19 $g{\cdot}cm^{-3}$) used for this intercomparison. The cuboid phantom has a 5 mm (diameter) by 10.4 mm (length) central cylindrical cavity to simultaneously house three TLDs, two alanine pellets, and six laser-cut films (see Fig. S3 as well). Section "Dosimetric systems" provides further information about the dosimeters. The dosimeter section was compressed by two nylon screws to ensure a reproducible geometry and minimize air gaps. A rectangular film was fixed on the cuboid phantom surface corresponding to the beam entrance to check dose homogeneity (Fig. 1).

The system is designed to be transported using standard mail and we have dedicated cuboid phantoms for monitoring dose during transport, as well as monitoring dose at the participating experimental sites.

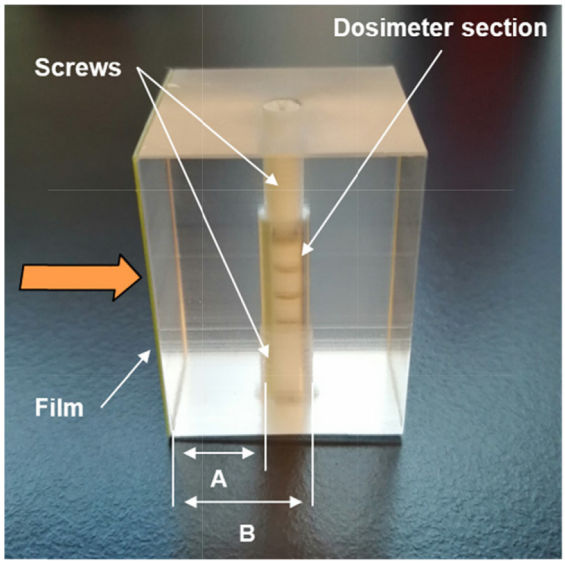

Fig. 1. Picture of the cuboid phantom showing the central dosimeter cavity loaded with dosimeters. The beam enters through the side of the cuboid phantom (orange arrow), which is covered by film. The depth of the dosimeters is defined by the physical lengths A and B.

Depth scaling

As the cuboid phantom material was not water-equivalent, the depths were scaled according to the international recommendations for electron beams from the Technical Reports Series (TRS) no. 398 (International Atomic Energy Agency) to convert PMMA depths into water equivalent depths [15]. Based on the TRS 398 methodology, each dosimeter's depth in the cuboid phantom was scaled and converted into its equivalent depth in water.

Dosimetric systems

The comparison scheme is based on the dosimetric studies performed at CHUV over the years [17,18]. It reflects the dosimetric procedure implemented routinely for radiobiological studies.

Alanine dosimetry was performed with 4.9 mm diameter and 3 mm thick pellets, read using a Bruker EPR spectrometer (Bruker Corporation, Billerica, Massachusetts, USA). The acquisition parameters were optimized for the dose range of 10–100 Gy for a dose uncertainty within ±2% (coverage factor k = 1[27]) to the actual dose using three repeated readouts [28]. The dosimeter was also calibrated in the electron beam of a Synergy medical LINAC (Elekta, Crawley, UK) against an ionization chamber traceable to the primary standard, a water calorimeter, of the Swiss Institute of Metrology (METAS).

For TLDs, we used round TLD-100 LiF:Mg,Ti chips (Thermo Fisher, USA) with a diameter of 4.5 mm and a thickness of 0.9 mm. Each TLD is individually calibrated in terms of absorbed dose to water with a Co-60 unit located at the institute of radiation physics (Lausanne, Switzerland) and also traceable to the primary standard of METAS [29]. The reading procedure as well as correction factors for electrons have been described in Jaccard *et al* and led to an overall uncertainty of 2.9% (k = 1) [18].

EBT3 Gafchromic films (Ashland Specialty Ingredients, Bridgewater, NJ, USA) were read with an EPSON V800 flatbed scanner (Epson America, Inc. Long Beach, CA, USA). A Trotec Speedy 300 2D laser cutting machine (Trotec Laser GmbH, Marchtrenk, Austria) was used to cut film disks of 5 mm diameter which were marked to indicate the orientation of the film. Film disks were then calibrated in terms of absorbed dose to water with the Synergy

medical LINAC using an 8 MeV electron beam traceable to international standards as described elsewhere [18]. All films were scanned sy-stematically-one week after irradiation to allow the return of the cuboid phantoms by mail. All image files were than analyzed with Mephysto software (PTW-Freiburg GmbH, Freiburg, Germany) for film calibration. The resulting uncertainty in dose measurements was 2% (k = 1) [18].

Irradiation procedure

The foreseen irradiation protocol contained information regarding the cuboid phantom and the water-equivalent depths of the dosimeters. This procedure was designed to guide test participants because of the potential high variability in the characteristics of the UHDR beams, such as in beam geometry or depth dose distribution. We present here the main guidelines of the procedure, which was sent to Stanford in order to test its feasibility.

Even though our detection system doesn't strongly depend on the primary electron beam mean energy, we reported beam parameters. We calculated the mean electron energy at the surface of the cuboid phantom using ICRU 35 recommendations. The field size and spectrum requirements are clearly not fulfilled, due to the requirements to obtain UHDR. However, we chose this indicator due to its clinical use and the lack of a better quantity. We calculated the mean electron energy by multiplying the half value depth (R50) by 2.33 MeV/cm according to ICRU 35. A detailed description of the eRT6 beam can be found in [34].

The beam entrance was indicated by the rectangular face of the cuboid phantom covered by a film and the beam had to be perpendicular to this surface (Fig. 1). Due to the limited dose ranges of the detectors, the optimum expected absorbed dose to water is between 7.5 and 16 Gy onto the cuboid phantom's central axis (in the middle of the dosimeters) as uniformly as possible. We reported the expected the minimum, average, and maximum dose within the section containing dosimeters according to the procedure described in the supplementary material. In addition to the cuboid phantoms used for irradiation, a supplementary cuboid phantom filled with dosimeters was sent for background monitoring. After the irradiation, the cuboid phantoms were sent back and the dosimeters were read at CHUV according to the procedures described in Section "Dosimetric systems".

Intercomparison pilot studies

The range of tested facilities and locations was designed to validate various aspects of the comparison scheme and ensure a smooth transition to an extended scheme in the near future.

First, irradiations were performed with three different devices at two different institutions on different continents to test for an international comparison. The first device was the Synergy medical LINAC (Elekta) at CHUV with a transmission chamber traceable to METAS for irradiations at CONV dose-rate. The second device was the Oriatron eRT6 (PMB-Alcen, France) at CHUV, a prototype LINAC involved in multiple FLASH preclinical studies as well as the first patient treatment with FLASH-RT [5,13,30–33]. This LINAC is able to perform irradiations with doses-per-pulse ranging from CONV ($\sim$ mGy) up to UHDR (>1 Gy) with microsecond pulse durations and does not have flattening filter [34]. The dosimetry, geometry and beam parameters are representative of the preclinical studies performed regularly at CHUV [17]. The last device included in this study was a Varian Trilogy medical LINAC (Varian Medical Systems, Inc., Palo Alto, CA) at Stanford. This device was used in clinical mode for CONV dose-rate irradiations but was configured as described elsewhere [12,35,36] for irradiations at UHDR. Setups for UHDR and CONV irradiations using this device are presented in Fig. 2A.

At Stanford, the cuboid phantoms were exposed to a 4 $\times$ 4 cm irradiation field (Fig. 2B), using a shield (leakage $\sim$ 1.5%) to shape the beam (Fig. 2C). The shield is a 3D printed hollow case filled with a 3 cm thick layer of aluminum oxide powder (265497, Sigma-Aldrich, USA) to stop electrons, and a 1 cm thick layer of 2 mm diameter tungsten spheres to stop Bremsstrahlung radiation (Fig. 2C). Fig. 2D shows the set-up developed using the eRT6. The beam is horizontal and the surface to source distances (SSDs) were chosen to optimize the dose per pulse. Finally, the Elekta Synergy set-up is shown in Fig. 2 E, and is equivalent to a clinical reference geometry, but using solid water.

For this first set of irradiations, three cuboid phantoms were irradiated in each available beam configuration (CONV or UHDR) on every device with a single beam. The detailed beam parameters and corresponding dose-rates from each irradiation are reported in Table 1. Typically, energy and field size were kept constant across the test and other beam parameters (SSD, pulse characteristics, and dose-per-pulse) were varied. This step is a robustness test of the comparisons scheme against beam geometry variations.

In addition, a larger test using 20 cuboid phantoms was performed on the Stanford system in order to evaluate our procedure against a wide range of beam parameters [12,35,36]. Phantom 19 was allocated for background measurement (remained with other cuboid phantoms), and phantom 20 for measurement of exposure during international transportation (remained in the shipping box).

A combination of ion chamber and film measurements were performed at Stanford to calibrate the system as well as to estimate the doses delivered to the dosimeter section in the center of the cuboid phantom, reported as the expected doses, for comparison with centralized readout of the dosimeters at CHUV, reported as the measured doses. A detailed description of the method is reported in the Supplementary Material.

Results

The depth scaling procedure given by the TRS 398 transformed the PDD measured in water into a water equivalent PDD measured in PMMA and enabled us to extract depth correction factors of approximately 11%. The depth scaling correction gave 11.1 mm instead of the original 10 mm for length A and 16.6 mm instead of 15 mm for length B (the physical dimensions of the cuboid phantom provided in the procedure are illustrated in Fig. 1).

We collected and averaged the measured dose values for the three tested LINACs, and Table 2 shows the average dose and the standard deviation (SD) of each set of dosimeters from the three cuboid phantoms and comparison with the expected doses. The standard deviation of the average doses given by each set of dosimeters in each configuration from the three cuboid phantoms remained below 3%. We also reported the relative bias, which is the ratio between the expected dose and the average measured dose, for each type of detector as well as an average over all types of detectors. Using clinical beam parameters, we found relative biases under 2%. When using UHDR beam parameters on the eRT6 and Trilogy, the relative biases increased, especially in the case of TLD.

The overall standard uncertainty on the dose measurements in CONV and UHDR were obtained by quadratic summation and found to be 5.1% for CONV and UHDR mode (Table 3).

The detailed results of beam parameters variation study are reported in the supplementary material (Table S2). We evaluated the internal consistency of our dosimeters and the accuracy of the measured dose at the center by calculating the relative bias to the alanine dose values, arbitrarily taken as reference, and as a function of the expected dose at center, Table 4 and Fig. 3. The average biases to the expected values are −0.90%, −7.45%, and

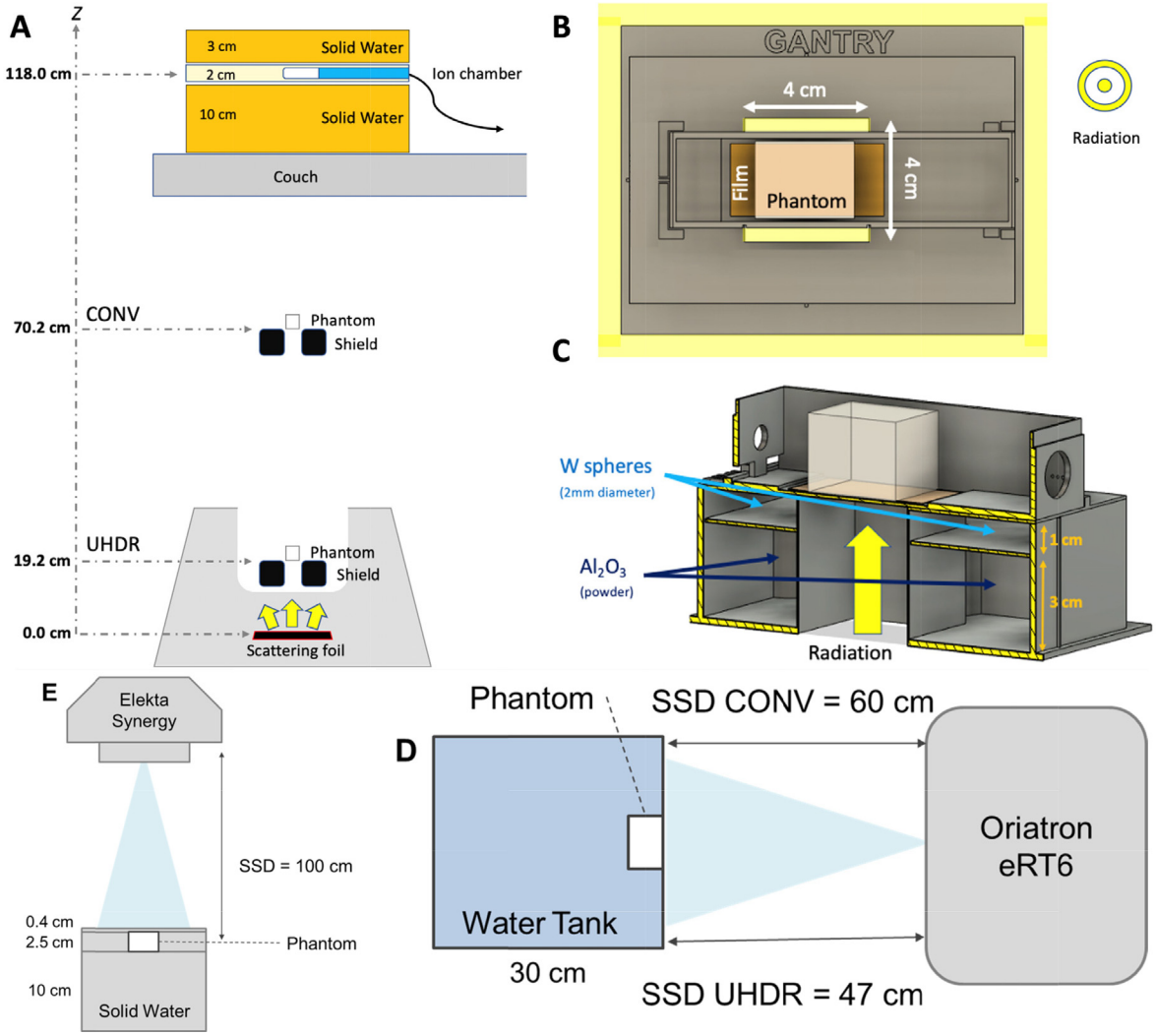

Fig. 2. Experimental setups with sample and shield geometry. (A) Schematic diagram of the Stanford setup illustrating the distance from the scattering foil for CONV versus UHDR irradiations. On the top, a solid water stack enclosed an ion chamber that measured the exit charge for each irradiation. (B) A top view of the shield and cuboid phantom setup, showing the placement of the cuboid phantom relative to the 4x4 cm opening in the shield forming the radiation field. In this view, the beam direction is out of the page. A film is placed at the entrance surface of the cuboid phantom in order to measure the entrance dose (C) The shield is a PLA 3D printed case, filled at the bottom with a 3 cm thick layer of aluminum oxide (Al_2O_3) powder and at the top with 1 cm thick layer of 2 mm diameter tungsten (W) spheres. (D) Set-up for the Oriatron eRT6 LINAC. (E) Clinical irradiation set-up using the Elekta Synergy.

Table 1
Conditions of the setup, beam, and the dose-rates used for the cuboid phantom irradiations during the test across accelerators and beam parameters at Stanford. Information regarding the latter is bolded.

	Elekta Synergy	Oriatron eRT6		Varian Trilogy	
Mode	CONV	CONV	UHDR	CONV	UHDR
Beam energy [MeV]	7.5	6	4.9	15.73/**15.73**	16.60/**16.60**
Field size [cm × cm]	20 × 20	10.5 (Ø)	9.6 (Ø)	4x4/**4x4**	4x4/**4x4**
SSD [cm]	100	60	47	82.2/**82.2**	19.2/**19.2**
Number of pulses	90,000	1070	3	9752/**4493, 8392**	10/**4, 5, 6, 7, 8, 10, 14**
Pulse repetition frequency [Hz]	400	10	100	72/**180**	90/**90**
Pulse width [μs]	3	1	2	5/**5**	5/**5**
Average dose-rate [Gy/s]	0.07	0.14	750	0.11/**0.30**	150/**95, 150, 200, 168, 240, 210, 420**
Dose-per-pulse [Gy]	0.00017	0.014	5	0.0015/**0.0017**	1.5/**1, 1.5, 2, 3.5**

−7.81% for alanine, TLD, and film respectively. The median biases are respectively −2.15%, −7.93%, and −7.78%. The plot on the right of Fig. 3 displays the biases for each detector type as a function of dose rate mode.

Finally, for all cuboid phantoms, we could determine that the reading of the central part of the film (15 × 10 mm^2) set on the entrance surface of the cuboid phantom shows an homogeneity compatible with the dosimeter overall uncertainties (k = 2).

Discussion

While the lack of traceability remains an inherent limitation of the current UHDR intercomparison study, our approach will

Table 2
Intercomparison results: Average dose from each dosimeter within the cuboid phantoms is reported together with the SD, minimum, average, and maximum doses to the dosimeters planned by the users. The relative bias between the expected dose and the average measured dose is also indicated.

	Elekta Synergy CONV		Oriatron eRT6 CONV		Oriatron eRT6 UHDR		Varian Trilogy CONV		Varian Trilogy UHDR	
Absorbed dose to water [Gy]	Average value	SD	Average value	SD	Average value	SD	Average value	SD	Average value	SD
Measured values										
TLD	14.7	0.2	14.8	0.2	13.4	0.3	14.4	0.1	13.7	0.4
EBT3	14.7	0.2	14.2	0.3	13.8	0.4	14.9	0.3	14.9	0.4
Alanine	14.9	0.1	14.4	0.4	13.9	0.3	15.1	0.2	14.6	0.1
Expected values										
Minimum	14.8		13.7		13.4		14.6		14.4	
Average	14.9		14.4		14.1		15.2		14.9	
Maximum	15.0		15.0		15.0		15.4		15.1	
TLD relative bias expected/measured dose [%]	−1.3		2.8		−5.0		−5.3		−8.1	
EBT3 relative bias expected/measured dose [%]	−1.3		−1.4		−2.1		−2.0		0.0	
Alanine relative bias expected/measured dose [%]	0.0		0.0		−1.4		−0.7		−2.0	
Average relative bias expected/measured dose [%]	−0.9		0.5		−2.8		−2.6		−3.4	

Table 3
Uncertainty budget: contribution on the absorbed dose to water measurements of the passive dosimeters.

Uncertainty contribution	u [%] (CONV)	u [%] (UHDR)
Calibration factor TLD	4.1	4.1
Calibration factor alanine	2	2
Calibration factor films	2	2
Positioning reproducibility	0.3	0.3
Output reproducibility	1	1

nonetheless foster greater consensus and repeatability between multicenter UHDR sites, representing an important step forward. Additionally, the methodology presented in this paper could be improved to future studies when a primary standard will be available.

In order to validate a comparison scheme tailored for UHDR accelerators, the feasibility of our strategy was studied in a first evaluation using various LINACS geometries, after which a stress test of our protocol against beam parameter variations was performed.

According to international guidelines, plastic phantoms are not recommended for absorbed dose determination in electron beams, but their use is permitted for nominal beam energies lower or equal to approximately 10 MeV. However we used electron beams up to 16 MeV in this work [15]. Other work has shown that the conversion factor from PMMA to water for electrons in the range of 1 to 50 MeV fluctuates by only about 1% and by less than 1% in the energy range of this work [37]. In addition, PMMA is transparent and well standardized, as well as simple to machine. As an initial step towards obtaining a dosimetric consensus, PMMA has proven to be adequate. However, if our scheme is needed for other beam types/qualities (*e.g.* protons) new materials could also be evaluated.

The first step of this study used a clinical LINAC with a CONV beam which provide an inherent validation in a well-controlled and standardized framework. The large beam size of the clinical Synergy LINAC 8 MeV electron beam provides a homogenous dose distribution across the dosimeter section, which resulted in expected relative biases (under 2%). That shows that the comparison scheme is compatible with CONV beam mode, which is a necessary precondition.

Then we investigated dose rate effects. In comparison to films and alanine, TLDs showed a stronger and systematic increase of relative biases when using UHDR beam parameters. For the Varian Trilogy and the eRT6, the TLDs biases between CONV and UHDR

Table 4
Intercomparison results: Relative bias of the results are presented in supplementary materials Table S2 as function of the alanine values, taken as reference, and as function of the expected dose.

Cuboid Cuboid phantom #	TLD Bias relative to Alanine %	Film Bias relative to Alanine %	Alanine Bias relative to Expected Dose %	TLD Bias relative to Expected Dose %	Film Bias relative to Expected Dose %
1	−6.62	−6.62	1.91	−4.71	−4.71
2	−6.61	−7.93	3.17	−3.44	−4.76
3	−4.96	−9.91	2.68	−2.28	−7.23
4	−6.38	−9.21	2.03	−4.35	−7.18
5	−4.27	−7.11	−1.88	−6.15	−8.99
6	−3.54	−5.67	−2.77	−6.31	−8.44
7	−5.69	−4.27	−4.08	−9.77	−8.35
8	−9.92	−6.61	−0.81	−10.73	−7.42
9	−13.22	−10.58	3.09	−10.13	−7.49
10	−10.60	−13.25	3.36	−7.24	−9.89
11	−4.63	−6.62	−3.30	−7.93	−9.92
12	−5.96	−7.95	−1.97	−7.93	−9.92
13	−2.85	−5.70	−2.32	−5.17	−8.02
14	−7.11	−7.11	−2.56	−9.67	−9.67
15	−7.44	−4.96	−3.35	−10.79	−8.31
16	−5.72	−3.58	−2.75	−8.47	−6.33
17	−4.32	−2.88	−4.35	−8.67	−7.23
18	−7.96	−4.34	−2.32	−10.28	−6.66

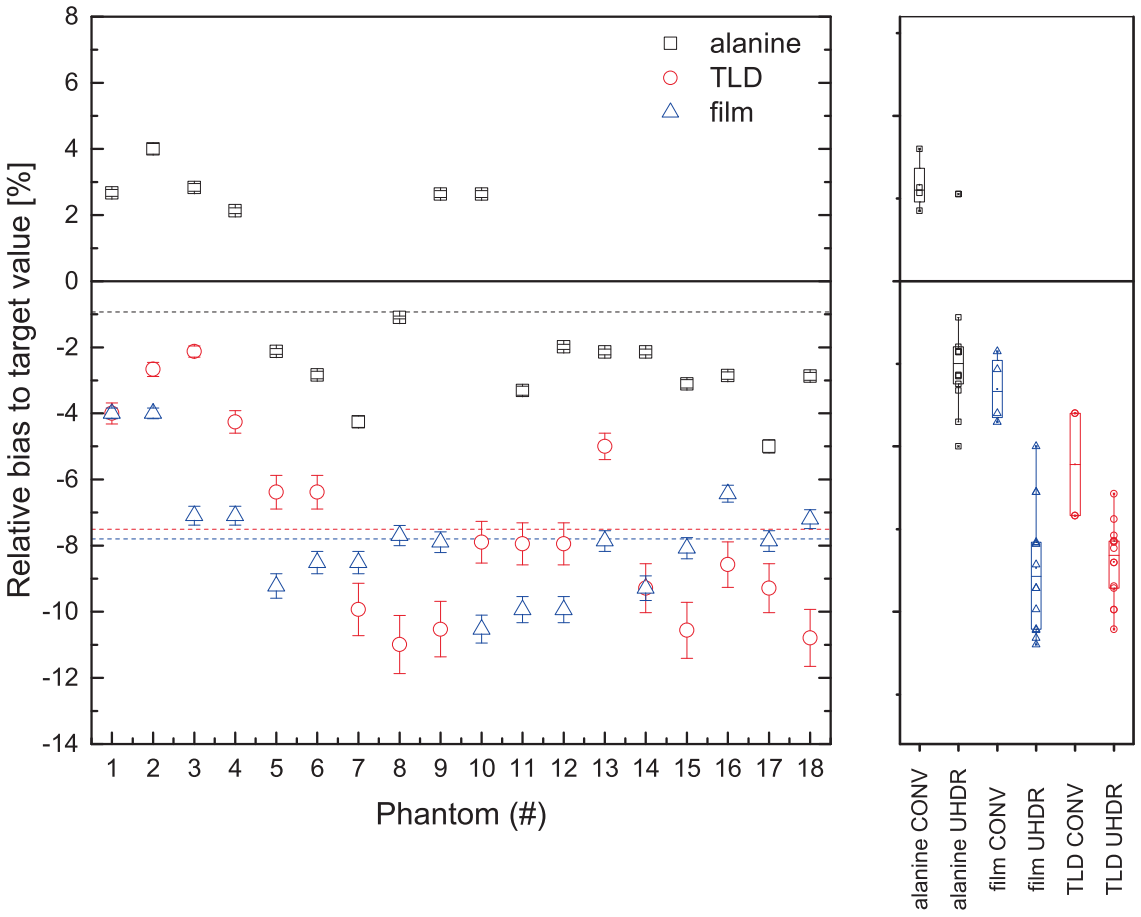

Fig. 3. Second round intercomparison results. Bias of the different detectors relative to the expected doses. The average bias is −0.90%, −7.45%, and −7.81% for alanine, TLD, and film, respectively. The right plot displays the biases for each detector and dose rate mode. There is a difference in the bias between CONV and UHDR measurements across all the detector types.

can be explained by a decrease in beam energy, which results in a difference in the energy correction factor. Consequently, it might indicate that the TLD energy correction factor should be adapted for such particular set-ups [18], even though the wide spectrum of the unfiltered beams might induce inevitable biases. Furthermore, such beam particularities are not reproduced at a calibration laboratory or a national metrology institute, which would make it impossible to base our investigations on an adequately calibrated instrument.

In addition, the large biases for the Varian Trilogy could suggest a strong geometric effect, which is different for the eRT6. Typically, the scattered beams are very different for large clinical beams and UHDR ones. The set-up at Stanford is different for CONV and UHDR, because the distance to the source is decreased for UHDR irradiations. The dose gradient and scattered beam component is logically different for both beam parameters, which induces discrepancies in beam characteristics. TLD detection efficiency is strongly dependent on photon energy in the range of hundreds of keV, which is taken into account using a well-defined calibration geometry with sufficient scattering medium in all directions. A difference between the scattered beam during calibrations (reference conditions) and comparisons could explain the observed effects.

Regarding Gafchromic films, the average dose was consistent with the alanine dosimeters within 2%. Even though films were selected for relative measurements, the accuracy was found to be adequate to support irradiation experiments and was typically used to record the entrance dose.

Finally, the low SDs from each dosimeter demonstrated a good reproducibility and homogeneity of the irradiations on each device. That was a particular concern using UHDR enhanced LINACs, which suffer from small beam sizes and bell-shaped lateral profiles.

We performed an evaluation of the robustness of the comparison scheme against beam parameters. In general, films and TLDs were in closer agreement with each other compared to alanine. Irradiations in CONV mode (cuboid phantoms 1 to 4) have relative biases of 2.45%, −3.70% and −5.97% for alanine, TLD and film respectively. These values are compatible with what was observed during the first tests. In UHDR mode, these biases are respectively −1.86%, −8.52% and −8.33%, which indicate a systematic underestimation of the measured doses in comparison to the expected doses. Alanine is in general closer to the expected dose, but due to the lack of absolute reference, it is impossible to gauge the accuracy. When looking at repeated irradiation parameters, we can deduce that the reproducibility of the measurement and the dose delivery is also adequate.

In conclusion, we have develop a scheme adequate to foster a dosimetric consensus between UHDR facilities. During this study, we were able to investigate the dosimetric consistency amongst two institutions, CHUV and Stanford, performing UHDR irradiations and found adequate consensus of dose predictions.

In the future, we plan to extend the procedure to other centers with other particle types such as protons or X-rays. Consequently, the cuboid phantom dimensions or material may be reconsidered to allow irradiation of the dosimeters in optimal setups.

Conclusion

We report an established and validated scheme for UHDR intercomparisons in order to bring dosimetry consensus across participating institutions. This method was tested and validated with high-energy electron beams between two centers and three different devices with CONV and UHDR. In addition, we tested the effect of beam parameters on the comparison agreement.

The compatibility between the measured and expected doses for all irradiations showed that dosimetry from both centers was in good agreement, which is a critical prerequisite for enabling preclinical experiments to be compared with experimental rigor and confidence.

This work is the first step towards a real multicenter intercomparison, thereby establishing a framework for other UHDR investigators in order to reach a UHDR dosimetric consensus.

Disclosure of conflicts of interest

BWL has received research support from Varian Medical Systems. BWL is a cofounder and board member of TibaRay.

Acknowledgement

We would like to thank Manuel Santos, Corinne Moratal and Sandrine Zufferey for their technical support (Institute of Radiation Physics, Switzerland).

We would like to thank Miguel Jimenez, Daniel Pawlak, and James Clayton from Varian Medical Systems for their technical assistance on the Trilogy FLASH irradiation configuration.

The study was supported by the grant P01CA244091 from the National Cancer Institute and the project 18HLT04 UHDpulse which has received funding from the EMPIR programme co-financed by the Participating States and from the European Union's Horizon 2020 research and innovation programme. Additional support was provided by the Stanford University Department of Radiation Oncology; the Weston Havens Foundation; the Stanford University School of Medicine; the Stanford University Office of the Provost; the Wallace H. Coulter Foundation; the Cancer League. We also gratefully acknowledge the generous support of philanthropic donors to the Department of Radiation Oncology at Stanford.

Appendix A. Supplementary material

Supplementary data to this article can be found online at https://doi.org/10.1016/j.radonc.2022.08.023.

References

[1] Cavedon C. Technical developments in high precision radiotherapy. Physica Med 2016;32:177.
[2] Prezado Y. [I147] New approaches in radiotherapy: spatial fractionation of the dose. Physica Med 2018;52:56.
[3] Berger T et al. Importance of technique, target selection, contouring, dose prescription, and dose-planning in external beam radiation therapy for cervical cancer: evolution of practice from EMBRACE-I to II. Int J Radiat Oncol Biol Phys 2019;104:885–94.
[4] Saberian F, Ghate A, Kim M. Optimal fractionation in radiotherapy with multiple normal tissues. Math Med Biol 2016;33:211–52.
[5] Montay-Gruel P et al. Irradiation in a flash: Unique sparing of memory in mice after whole brain irradiation with dose rates above 100Gy/s. Radiother Oncol 2017;124:365–9.
[6] Vozenin MC et al. The advantage of FLASH radiotherapy confirmed in mini-pig and cat-cancer patients. Clin Cancer Res 2018.
[7] Favaudon V et al. Ultrahigh dose-rate FLASH irradiation increases the differential response between normal and tumor tissue in mice. Sci Transl Med 2014;6:245ra93.
[8] Montay-Gruel P et al. X-rays can trigger the FLASH effect: Ultra-high dose-rate synchrotron light source prevents normal brain injury after whole brain irradiation in mice. Radiother Oncol 2018.
[9] Vozenin MC, Hendry JH, Limoli CL. Biological benefits of ultra-high dose rate FLASH radiotherapy: sleeping beauty awoken. Clin Oncol (R Coll Radiol) 2019;31:407–15.
[10] Fouillade C et al. FLASH irradiation spares lung progenitor cells and limits the incidence of radio-induced senescence. Clin Cancer Res 2019.
[11] Kim YE et al. Effects of ultra-high doserate FLASH irradiation on the tumor microenvironment in Lewis Lung Carcinoma: role of myosin light chain. Int J Radiat Oncol Biol Phys 2020.
[12] Levy K et al. Abdominal FLASH irradiation reduces radiation-induced gastrointestinal toxicity for the treatment of ovarian cancer in mice. Sci Rep 2020;10:21600.
[13] Montay-Gruel P et al. Long-term neurocognitive benefits of FLASH radiotherapy driven by reduced reactive oxygen species. Proc Natl Acad Sci U S A 2019;116:10943–51.
[14] International Atomic Energy Agency V. Radiation oncology physics: a handbook for teachers and students; 2005, International Atomic Energy Agency (IAEA): IAEA.
[15] International Atomic Energy Agency. Absorbed dose determination in external beam radiotherapy, technical reports series no. 398, IAEA, Vienna; 2000.
[16] Schüller A et al. The European Joint Research Project UHDpulse – Metrology for advanced radiotherapy using particle beams with ultra-high pulse dose rates. Physica Med 2020;80:134–50.
[17] Jorge PG et al. Dosimetric and preparation procedures for irradiating biological models with pulsed electron beam at ultra-high dose-rate. Radiother Oncol 2019;139:34–9.
[18] Jaccard M et al. High dose-per-pulse electron beam dosimetry: Usability and dose-rate independence of EBT3 Gafchromic films. Med Phys 2017;44:725–35.
[19] Karsch L et al. Dose rate dependence for different dosimeters and detectors: TLD, OSL, EBT films, and diamond detectors. Med Phys 2012;39:2447–55.
[20] Desrosiers MF, Publ JM, Cooper SL. An absorbed-dose/dose-rate dependence for the alanine-EPR dosimetry system and its implications in high-dose ionizing radiation metrology. J Res Nat Inst Stand Technol 2008;113:79–95.
[21] Desrosiers MF, Puhl JM. Absorbed-dose/dose-rate dependence studies for the alanine-EPR dosimetry system. Radiat Phys Chem 2009;78:461–3.
[22] Olsen KJ, Hansen JW, Wille M. Response of the alanine radiation dosimeter to high-energy photon and electron-beams. Phys Med Biol 1990;35:43–52.
[23] Tochilin E, Goldstein N. Dose rate and spectral measurements from pulsed X-ray generators. Health Phys 1966;12:1705.
[24] Karzmark CJ. Some aspects of lithium-fluoride thermoluminescence dosimetry. Phys Med Biol 1964;9:102–1000.
[25] Bourhis J et al. Clinical translation of FLASH radiotherapy: why and how? Radiother Oncol 2019;139:11–7.
[26] Vozenin MC et al. All Irradiations that are ultra-high dose rate may not be FLASH: the critical importance of beam parameter characterization and in vivo validation of the FLASH Effect AN INTRODUCTION LETTER. Radiat Res 2020;194:571–2.
[27] Taylor BN, Kuyatt CE. Guidelines for evaluating and expressing the uncertainty of NIST measurement results, vol. 1297. US Department of Commerce, Technology Administration, National Institute of . . .; 1994.
[28] Gondre M et al. Optimization of alanine measurements for fast and accurate dosimetry in FLASH radiation therapy. Radiat Res 2020;194:573–9.
[29] Stucki G, Muench W, Quintel H. The METAS absorbed dose to water calibration service for high energy photon and electron beam radiotherapy; 2002.
[30] Bourhis J et al. Treatment of a first patient with FLASH-radiotherapy. Radiother Oncol 2019;139:18–22.
[31] Alaghband Y et al. Neuroprotection of radiosensitive juvenile mice by ultra-high dose rate FLASH irradiation. Cancers (Basel) 2020;12.
[32] Allen BD et al. Maintenance of tight junction integrity in the absence of vascular dilation in the brain of mice exposed to ultra-high-dose-rate FLASH irradiation. Radiat Res 2020;194:625–35.
[33] Montay-Gruel P et al. Hypo-fractionated FLASH-RT as an effective treatment against glioblastoma that reduces neurocognitive side effects in mice. Clin Cancer Res 2020.
[34] Jaccard M et al. High dose-per-pulse electron beam dosimetry: commissioning of the Oriatron eRT6 prototype linear accelerator for preclinical use. Med Phys 2018;45:863–74.
[35] Schuler E et al. Experimental platform for ultra-high dose rate FLASH irradiation of small animals using a clinical linear accelerator. Int J Radiat Oncol Biol Phys 2017;97:195–203.
[36] Eggold JT et al. Abdominopelvic FLASH irradiation improves PD-1 immune checkpoint inhibition in preclinical models of ovarian cancer. Mol Cancer Ther 2021.
[37] FernandezVarea JM, Andreo P, Tabata T. Detour factors in water and plastic phantoms and their use for range and depth scaling in electron-beam dosimetry. Phys Med Biol 1996;41:1119–39.